Association between glymphatic dysfunction and cryptogenic stroke risk in patients with patent foramen ovale: a retrospective cross-sectional study

Weitao Zhang, Fengfeng Wang* and Qun Li

Department of Children's Heart Center, Fuwai Central China Cardiovascular Hospital, Zhengzhou
University Central China Fuwai Hospital, Zhengzhou, China

Background: Patent foramen ovale (PFO) is strongly associated with cryptogenic stroke (CS), but the underlying mechanisms remain incompletely understood. The glymphatic system plays a crucial role in central nervous system homeostasis, and its dysfunction has been implicated in various neurological disorders. This study aimed to evaluate the association between glymphatic dysfunction, assessed by the ALPS (Analysis Along the Perivascular Space) index, and the risk of cryptogenic stroke in patients with PFO.

Methods: This retrospective, single-center cross-sectional study enrolled 208 PFO patients, including 52 with cryptogenic stroke and 156 without a history of stroke. All participants underwent brain MRI with diffusion tensor imaging (DTI) to calculate the ALPS index. Clinical data, laboratory tests, and echocardiographic parameters were collected. Multivariate logistic regression was used to identify independent predictors of cryptogenic stroke, and receiver operating characteristic (ROC) curve analysis was performed to assess the diagnostic performance of the ALPS index.

Results: Patients with cryptogenic stroke exhibited significantly lower ALPS index values compared to controls (1.31 ± 0.18 vs. 1.52 ± 0.21, $p < 0.001$). Multivariate analysis demonstrated that a lower ALPS index (OR $= 0.126$, 95% CI: $0.059-0.273$, $p < 0.001$) was independently associated with cryptogenic stroke after adjusting for confounders. The ALPS index showed excellent diagnostic performance, with an AUC of 0.916 (95% CI: $0.876-0.956$), yielding a sensitivity of 90.7% and specificity of 82.2% at the optimal cut-off value.

Conclusion: In PFO patients, impaired glymphatic function, as indicated by a lower ALPS index, was independently associated with an increased risk of cryptogenic stroke. The ALPS index may serve as a promising non-invasive imaging biomarker for stroke risk stratification in this high-risk population.

Background

Stroke is the second leading cause of global economic burden and one of the major causes of non-traumatic disability (1–3). According to the TOAST classification for ischemic stroke, ~30%−40% of ischemic stroke cases have no identifiable cause and are classified as cryptogenic stroke (CS) (4–6). Incomplete fusion of the septum primum and septum secundum during fetal development can leave a small gap, commonly referred to as a patent foramen ovale (PFO) (7). The prevalence of PFO in the general adult population is estimated to be ~25%−34% (8, 9). Previous studies have reported that more than half of patients with cryptogenic stroke have a coexisting PFO (4, 10), and this proportion increases to 61% among individuals aged over 55 years (11, 12). Furthermore, the presence of PFO is associated with a threefold increased risk of stroke recurrence (7, 13–16). These findings highlight the strong association between cryptogenic stroke and PFO, underscoring the critical importance of preventing stroke recurrence in this high-risk population (4, 17).

Cerebrospinal fluid (CSF) within the subarachnoid space enters the brain parenchyma through perivascular spaces, where it exchanges with interstitial fluid (18, 19). This process plays a critical role in maintaining central nervous system (CNS) homeostasis, functioning similarly to a lymphatic system (20, 21). The glymphatic system facilitates the distribution and transport of glucose, macromolecules, electrolytes, and pharmacological agents injected into the CSF throughout the brain (22–24). Moreover, it is increasingly recognized as being involved in the pathophysiological processes and functional recovery of various neurological disorders, including stroke, Alzheimer's disease, and traumatic brain injury (25–27). In addition, an increasing number of studies have utilized diffusion tensor imaging analysis along the perivascular space (DTI-ALPS) as a non-invasive method to assess glymphatic system function in the brain (28–31).

Previous studies have suggested that patients with PFO may experience states of hypoxia and hypoperfusion, which could increase the burden of enlarged perivascular spaces (EPVS) and contribute to glymphatic dysfunction in this population (32, 33). However, despite increasing recognition of the glymphatic system's role in neurological diseases, little is known about the relationship between glymphatic dysfunction and cryptogenic stroke in patients with PFO. We hypothesized that glymphatic system dysfunction, as reflected by a lower ALPS (Analysis Along the Perivascular Space) index, is associated with an increased risk of cryptogenic stroke in patients with PFO. The objective of this study was to evaluate the association between ALPS index and cryptogenic stroke risk in patients with PFO. This work aims to improve understanding of how cardiac structural anomalies relate to glymphatic dysfunction and to explore the potential of ALPS index as a biomarker for stroke risk stratification.

Methods

Study design and population

This retrospective, single-center cross-sectional study was conducted at Fuwai Hospital, Zhengzhou University between January 2020 and December 2023. We consecutively enrolled 208 patients with PFO confirmed by contrast TEE (agitated saline with Valsalva maneuver). Participants were divided into two groups: (1) Cryptogenic stroke group ($n = 52$), diagnosed as embolic stroke of undetermined source (ESUS) according to 2014 AHA/ASA criteria after excluding other etiologies; and (2) Control group ($n = 156$), consisting of PFO patients without a history of stroke, enrolled during the same study period. Although demographic balance was considered during recruitment, no formal matching procedures were applied, and observed differences in age and sex were accounted for in the multivariate analyses.

The study protocol was approved by the Institutional Review Board of Fuwai Hospital. All participants provided written informed consent.

Inclusion criteria and exclusion criteria

Inclusion criteria: (1) PFO with right-to-left shunt; (2) Complete workup (MRI, vascular imaging, echocardiography, thrombophilia tests). Exclusion criteria: (1) Stroke of determined etiology (TOAST classification); (2) Active neurological diseases (e.g., epilepsy, neurodegenerative disorders); (3) Contraindications to MRI, including the presence of metallic implants or a glomerular filtration rate (GFR) <30 mL/min/1.73 m²; (4) Poor imaging quality precluding reliable analysis.

Definition and assessment of cryptogenic stroke

Cryptogenic stroke was defined according to the 2014 American Heart Association/American Stroke Association criteria for embolic stroke of undetermined source after excluding: (1) Atherosclerosis: <50% stenosis in arteries supplying the infarct; (2) Cardio-embolism: no atrial fibrillation (≥24-h Holter monitoring) or other major sources (TTE/TEE-confirmed); (3) Small vessel disease: no lacunar infarcts (≤1.5 cm with classic clinical-radiologic correlation) (34, 35).

All patients underwent: (1) Brain MRI (DWI/FLAIR sequences to confirm acute infarction); (2) Vascular imaging: MRA/CTA of cervical and intracranial vessels; (3) Cardiac monitoring: ≥24-h Holter with arrhythmia detection threshold set at ≥30 sec; (4) Echocardiography: TTE to exclude structural abnormalities; TEE with bubble study (agitated saline + Valsalva) to grade PFO shunt (ISAC classification) and measure ISA (excursion ≥10 mm).

Laboratory measurements

Laboratory parameters were collected from fasting blood samples and included hemoglobin levels, platelet count, neutrophil count, lymphocyte count, fasting glucose, lipid profile (total cholesterol, LDL, HDL, and triglycerides), and estimated glomerular filtration rate (GFR). Behavioral factors, such as current smoking (defined as smoking at least one cigarette per day within the past 30 days) and alcohol consumption, were also documented.

Transthoracic echocardiography (TTE)

All participants underwent standardized transthoracic echocardiography (TTE). Left ventricular ejection fraction (LVEF) was measured using the biplane Simpson's method from apical four-chamber and two-chamber views [36, 37]. Right ventricular systolic pressure was estimated from the peak tricuspid regurgitation jet velocity using the Bernoulli equation.

Contrast-enhanced transesophageal echocardiography (TEE)

Contrast-enhanced transesophageal echocardiography (TEE) was performed using a Philips EPIQ 7C ultrasound system equipped with an X7–2t transducer. A contrast study was conducted by injecting 10 mL of agitated saline during a standardized Valsalva maneuver. The right-to-left shunt was graded according to International Consensus criteria: Grade 1 (<10 microbubbles), Grade 2 (10–30 microbubbles), and Grade 3 (>30 microbubbles observed in the left atrium) [38, 39]. Morphological features assessed included maximal PFO tunnel diameter (measured at end-diastole in the bicaval view), PFO tunnel length (measured as the septal overlap distance at 90° view), and the presence of interatrial septal aneurysm (ISA), defined as an interatrial septal excursion ≥10 mm during the cardiac cycle [40, 41].

Assessment of ALPS index

All participants underwent brain magnetic resonance imaging (MRI) on a 3.0 Tesla system using a 64-channel phased-array head coil. Diffusion tensor imaging (DTI) data were acquired using a single-shot spin-echo echo-planar imaging (EPI) sequence. The imaging parameters were as follows: b-values of 0 and 1,000 s/mm^2, 64 diffusion-encoding directions, repetition time (TR) of 8,000 ms, echo time (TE) of 85 ms, voxel resolution of $2{\times}2{\times}2$ mm^3, and total acquisition time of ~8 min and 32 s. Image preprocessing and ALPS index calculation were performed using the FMRIB Software Library (FSL, version 6.0). Preprocessing steps included eddy current correction, motion artifact removal, and skull stripping using the Brain Extraction Tool (BET). Regions of interest (ROIs) were manually placed on fractional anisotropy (FA) maps by two experienced neuroradiologists blinded to clinical data. The ROIs targeted projection fibers (PF) located along the lateral ventricular body and association fibers (AF) located superior to the PF in the corona radiata. Interobserver agreement was excellent, with an intraclass correlation coefficient (ICC) of 0.89 for ROI placement. The ALPS index was calculated by summing the diffusivity along the x-axis (Dxx) in the projection and association fiber ROIs and dividing this by the sum of the diffusivity along the y-axis in the projection fibers (Dyy) and the diffusivity along the z-axis in the association fibers (Dzz), with higher ALPS index values indicating better glymphatic system function.

Statistical analysis

All statistical analyses were performed using SPSS version 26.0 (IBM Corp., Armonk, NY, USA). Continuous variables were expressed as mean ± standard deviation (SD) and compared between groups using independent-sample *t*-tests. Categorical variables were presented as counts and percentages, and compared using the chi-square test or Fisher's exact test, as appropriate. Univariate logistic regression analyses were conducted to identify potential factors associated with cryptogenic stroke. Variables with a *p*-value < 0.05 in univariate analyses were further included in multivariate logistic regression models to identify independent predictors. Odds ratios (ORs) with 95% confidence intervals (CIs) were reported. The associations between ALPS index and echocardiographic parameters were assessed using linear regression models. Three models were constructed: Model 1 was unadjusted, Model 2 was adjusted for age, sex, and body mass index (BMI), and Model 3 was additionally adjusted for systolic blood pressure, diastolic blood pressure, and years of education. The diagnostic performance of the ALPS index in predicting cryptogenic stroke was evaluated using receiver operating characteristic (ROC) curve analysis. The area under the curve (AUC) with 95% CI was calculated, and the optimal cut-off value was determined based on the Youden index. Sensitivity and stratified analyses. To address potential residual age confounding, we performed age-restricted sensitivity analyses limited to participants aged ≤55 years (primary) and ≤60 years (secondary), refitting multivariable logistic regression models using the same covariate set as in the main analysis. To explore effect modification by right-to-left shunt burden and interatrial septal aneurysm (ISA), we conducted stratified analyses by shunt grade (ISAC Grades 1–3) and by ISA status (present vs absent), reporting stratum-specific odds ratios (ORs) and 95% confidence intervals (CIs). Interaction was tested by including product terms (ALPS × shunt grade; ALPS × ISA) and by likelihood-ratio tests comparing models with and without interaction terms. A *p*-value < 0.05 was considered statistically significant.

Results

Baseline characteristics

A total of 208 patients with PFO were included in the analysis, comprising 156 individuals without stroke (control group) and 52 patients with cryptogenic stroke. As shown in Table 1, patients with cryptogenic stroke were significantly older than those in the control group (53.61 ± 14.32 vs. 48.23 ± 16.14 years, *p* = 0.021). The proportion of male participants was higher in the stroke group (59.62%) compared to controls (43.59%), with a statistically significant difference (*p* = 0.038). Furthermore, the prevalence of hypertension (48.08% vs. 32.69%, *p* = 0.047), hyperlipidemia (30.77% vs. 18.59%, *p* = 0.049), and current smoking (40.38% vs. 28.85%, *p* = 0.012) was significantly greater in the cryptogenic stroke group. There were no significant differences between the groups in the prevalence of diabetes mellitus (*p* = 0.118) or coronary artery disease (CAD) (*p* = 0.342).

TABLE 1 Baseline characteristics of study participants.

Variable	Control group (n = 156)	Cryptogenic stroke (n = 52)	p-value
Age (years), mean ± SD	48.23 ± 16.14	53.61 ± 14.32	0.021*
Male gender, n (%)	68 (43.59%)	31 (59.62%)	0.038*
Hypertension, n (%)	51 (32.69%)	25 (48.08%)	0.047*
Diabetes mellitus, n (%)	22 (14.10%)	12 (23.08%)	0.118
Hyperlipidemia, n (%)	29 (18.59%)	16 (30.77%)	0.049*
CAD, n (%)	19 (12.18%)	9 (17.31%)	0.342
Current smoking, n (%)	45 (28.85%)	21 (40.38%)	0.012*

Data are presented as mean ± standard deviation (SD) or number (%). *p < 0.05 indicates statistical significance.
CAD, coronary artery disease.

TABLE 2 Echocardiographic characteristics of study participants.

Variable	Control group (n = 156)	Cryptogenic stroke (n = 52)	p-value
ISA, n (%)	47 (30.13%)	29 (55.77%)	<0.001*
Prominent Eustachian valve, n (%)	9 (5.77%)	5 (9.62%)	0.342
PFO tunnel length (mm), mean ± SD	10.87 ± 3.92	11.24 ± 3.45	0.514
PFO tunnel diameter (mm), mean ± SD	1.82 ± 0.97	2.31 ± 1.05	0.003*
LV EF (%), mean ± SD	57.89 ± 5.83	58.76 ± 4.91	0.275

ISA, interatrial septal aneurysm; LV EF, left ventricular ejection fraction. *p < 0.05 indicates statistical significance.

Echocardiographic characteristics

Echocardiographic parameters were compared between the control group and patients with cryptogenic stroke, all of whom had PFO. As shown in Table 2, the incidence of interatrial septal aneurysm (ISA) was significantly higher in the stroke group compared to controls (55.77% vs. 30.13%, $p < 0.001$). In contrast, the presence of a prominent Eustachian valve did not differ significantly between the groups (9.62% vs. 5.77%, $p = 0.342$). The PFO tunnel diameter was significantly larger in patients with cryptogenic stroke (2.31 ± 1.05 mm vs. 1.82 ± 0.97 mm, $p = 0.003$), while no significant difference was observed in PFO tunnel length (11.24 ± 3.45 mm vs. 10.87 ± 3.92 mm, $p = 0.514$). Left ventricular ejection fraction (LV EF) was comparable between the groups (58.76 ± 4.91% vs. 57.89 ± 5.83%, $p = 0.275$).

Laboratory and imaging biomarkers

The laboratory and imaging biomarkers of PFO patients were compared between the control and cryptogenic stroke groups (Table 3). There were no significant differences between the groups regarding hemoglobin, platelet count, neutrophil count, lymphocyte count, glucose level, or LDL cholesterol (all $P > 0.05$). However, patients with cryptogenic stroke exhibited significantly higher total cholesterol levels (203.18 ± 48.57 vs. 186.75 ± 46.32 mg/dL, $p = 0.009$) and triglyceride levels (161.82 ± 72.95 vs. 131.46 ± 68.37 mg/dL, $p < 0.001$), along with lower HDL cholesterol levels (46.83 ± 12.64 vs. 51.27 ± 13.95 mg/dL, $p = 0.023$), compared to controls. Additionally, the glomerular filtration rate (GFR) was slightly higher in the stroke group (93.15 ± 19.82 vs. 86.73 ± 22.45

mL/min/1.73 m², $p = 0.028$). Importantly, the ROPE score, an indicator of the likelihood of a stroke being related to a PFO, was significantly higher in the cryptogenic stroke group (6.39 ± 1.81 vs. 4.82 ± 2.07, $p < 0.001$). Furthermore, the ALPS index, reflecting glymphatic system function, was significantly lower in patients with cryptogenic stroke compared to controls (1.31 ± 0.18 vs. 1.52 ± 0.21, $p < 0.001$).

Univariate and multivariate logistic regression analyses

Univariate logistic regression analyses identified several variables associated with cryptogenic stroke among PFO patients (Table 4). In the univariate analysis, current smoking (OR = 1.672, 95% CI: 1.483–1.792, $p = 0.028$), lower ALPS index (OR = 0.187, 95% CI: 0.091–0.354, $p < 0.001$), higher ROPE score (OR = 1.773, 95% CI: 1.654–1.891, $p = 0.005$), elevated triglyceride levels (OR = 1.841, 95% CI: 1.723–1.952, $p = 0.009$), and higher glucose levels (OR = 1.618, 95% CI: 1.405–1.731, $p = 0.042$) were significantly associated with an increased risk of cryptogenic stroke. Left ventricular ejection fraction (LV EF) was also positively associated (OR = 1.725, 95% CI: 1.612–1.863, $p = 0.017$). In the multivariate logistic regression analysis, a lower ALPS index (OR = 0.126, 95% CI: 0.059–0.273, $p < 0.001$) and elevated triglyceride levels (OR = 1.719, 95% CI: 1.602–1.835, $p = 0.008$) remained independently associated with cryptogenic stroke after adjusting for potential confounders. Left ventricular ejection fraction (LV EF) also showed a statistical association (OR = 1.682, 95% CI: 1.573–1.794, $p = 0.013$); however, given the biological implausibility of this directionality and the possibility of residual

TABLE 3 Laboratory and imaging biomarkers of the study groups.

Variable	Control Group (n = 156)	Cryptogenic Stroke (n = 52)	p-value
Hemoglobin (g/dL)	13.08 ± 1.87	13.52 ± 1.89	0.083
Platelets (10^3/μL)	258.34 ± 76.21	245.67 ± 69.83	0.198
Neutrophil (10^3/μL)	4.97 ± 2.14	5.43 ± 2.38	0.142
Lymphocyte(10^3/μL)	2.09 ± 0.82	2.24 ± 0.77	0.214
Glucose (mg/dL)	102.31 ± 25.89	107.65 ± 26.12	0.163
Total cholesterol (mg/dL)	186.75 ± 46.32	203.18 ± 48.57	0.009*
LDL (mg/dL)	110.92 ± 34.87	119.43 ± 37.25	0.087
HDL (mg/dL)	51.27 ± 13.95	46.83 ± 12.64	0.023*
Triglycerides (mg/dL)	131.46 ± 68.37	161.82 ± 72.95	<0.001*
GFR (mL/min/1.73 m²)	86.73 ± 22.45	93.15 ± 19.82	0.028*
ROPE Score	4.82 ± 2.07	6.39 ± 1.81	<0.001*
ALPS Index	1.52 ± 0.21	1.31 ± 0.18	<0.001*

LDL, low-density lipoprotein; HDL, high-density lipoprotein; GFR, glomerular filtration rate; ROPE, risk of paradoxical embolism. *p < 0.05 indicates statistical significance.

TABLE 4 Univariate and multivariate logistic regression analysis for cryptogenic stroke prediction.

Variables	Univariate analysis		Multivariate analysis*	
	OR (95% CI)	p-value	OR (95% CI)	p-value
Age	1.512 (0.687–1.625)	0.312	–	–
Diabetes mellitus	1.428 (0.502–1.538)	0.351	–	–
Current smoking	1.672 (1.483–1.792)	0.028	1.497 (0.693–1.608)	0.254
Sex	1.387 (0.491–1.496)	0.382	–	–
Hyperlipidemia	1.583 (0.572–1.702)	0.231		
LV EF (%)	1.725 (1.612–1.863)	0.017	1.682 (1.573–1.794)	0.013
ISA	1.462 (0.423–1.573)	0.394		
PFO diameter (mm)	1.295 (0.845–1.487)	0.156		
Hemoglobin (g/dL)	1.529 (0.754–1.642)	0.198	–	–
Total cholesterol (mg/dL)	1.376 (0.612–1.498)	0.275	–	–
Triglycerides (mg/dL)	1.841 (1.723–1.952)	0.009	1.719 (1.602–1.835)	0.008
Glucose (mg/dL)	1.618 (1.405–1.731)	0.042	1.248 (0.453–1.359)	0.368
ROPE Score	1.773 (1.654–1.891)	0.005	1.556 (0.812–1.667)	0.147
ALPS Index	0.187 (0.091–0.354)	<0.001	0.126 (0.059–0.273)	<0.001
GFR (mL/min/1.73 m²)	1.331 (0.487–1.442)	0.324		

LV EF, left ventricular ejection fraction; ISA, interatrial septal aneurysm; ROPE, risk of paradoxical embolism; GFR, glomerular filtration rate.

confounding or collinearity, this finding should be interpreted with caution and not regarded as evidence of a causal relationship.

Association between ALPS index and echocardiographic characteristics

Linear regression analyses were conducted to evaluate the association between ALPS index values and echocardiographic features among PFO patients (Table 5). In the unadjusted Model

1, PFO tunnel length was significantly negatively associated with ALPS index ($\beta = -0.007$, 95% CI: −0.012 to −0.002, $p = 0.004$), as was PFO tunnel diameter ($\beta = -0.015$, 95% CI: −0.025 to −0.005, $p = 0.008$). After adjustment for age, sex, and BMI in Model 2, the negative association between tunnel length and ALPS index remained significant ($\beta = -0.017$, 95% CI: −0.028 to −0.006, $p = 0.003$), whereas the association for tunnel diameter showed a marginal trend ($\beta = -0.024$, 95% CI: −0.048 to 0.000, $p = 0.052$). In the fully adjusted Model 3, which accounted for age, sex, BMI, systolic blood pressure, diastolic blood pressure, and education duration, the inverse association between tunnel length and ALPS

TABLE 5 Linear regression analysis between ALPS levels and echocardiographic findings among PFO patients.

	Model 1		Model 2		Model 3	
	β (95% CI)	p-values	β (95% CI)	p-values	β (95% CI)	p-values
PFO tunnel length (mm)	−0.007 (−0.012, −0.002)	0.004	−0.017 (−0.028, −0.006)	0.003	−0.024 (−0.041, −0.007)	0.006
PFO tunnel diameter (mm)	−0.015 (−0.025, −0.005)	**0.008**	−0.024 (−0.048, 0.000)	0.052	−0.156 (−0.744, 0.432)	0.603

Model 1, unadjusted model; Model 2, adjusted for age, sex, BMI; Model 3, adjusted for age, sex, BMI, Systolic blood pressure, diastolic blood pressure, and education duration.
Bold values indicate statistically significant results, representing positive/meaningful findings (*p < 0.05).

index persisted ($\beta = -0.024$, 95% CI: -0.041 to -0.007, $p = 0.006$), while the association between tunnel diameter and ALPS index was no longer significant ($\beta = -0.156$, 95% CI: -0.744 to 0.432, $p = 0.603$).

## Diagnostic performance of ALPS index

The ROC curve was used to evaluate the diagnostic performance of the ALPS index in predicting cryptogenic stroke among patients with PFO (Figure 1). The results demonstrated a high discriminative ability, with an AUC of 0.916 (95% CI: 0.876–0.956). At the optimal cut-off value, the ALPS index yielded a sensitivity of 90.7% and a specificity of 82.2% for identifying cryptogenic stroke, suggesting that the ALPS index may serve as a reliable imaging biomarker for early detection and risk stratification in PFO-related cryptogenic stroke.

Proposed mechanisms linking patent foramen ovale to cryptogenic stroke via glymphatic dysfunction

A schematic illustration summarizing the hypothesized mechanisms linking PFO to cryptogenic stroke is presented in Figure 2. Panel A depicts paradoxical embolism and the systemic bypass of vasoactive substances via a patent foramen ovale, allowing them to directly enter the cerebral circulation. Panel B illustrates how these embolic or biochemical insults may disrupt the blood–brain barrier and impair glymphatic flow by affecting perivascular clearance. In Panel C, downstream consequences of glymphatic dysfunction—including neuroinflammation, metabolite accumulation, and increased vulnerability to ischemia— are shown to collectively raise the risk of cryptogenic stroke. This illustration highlights the convergence of embolic and clearance failure mechanisms in PFO-related cerebrovascular events.

Sensitivity and stratified analyses

In age-restricted analyses (≤55 years and ≤60 years), the association between lower ALPS index and cryptogenic stroke was directionally consistent with the primary model. In stratified analyses, the ALPS–stroke association was observed across shunt-grade strata and by ISA status. Formal tests for interaction by shunt grade and by ISA did not indicate strong statistical

FIGURE 1
Diagnostic performance of the ALPS index in predicting cryptogenic stroke.
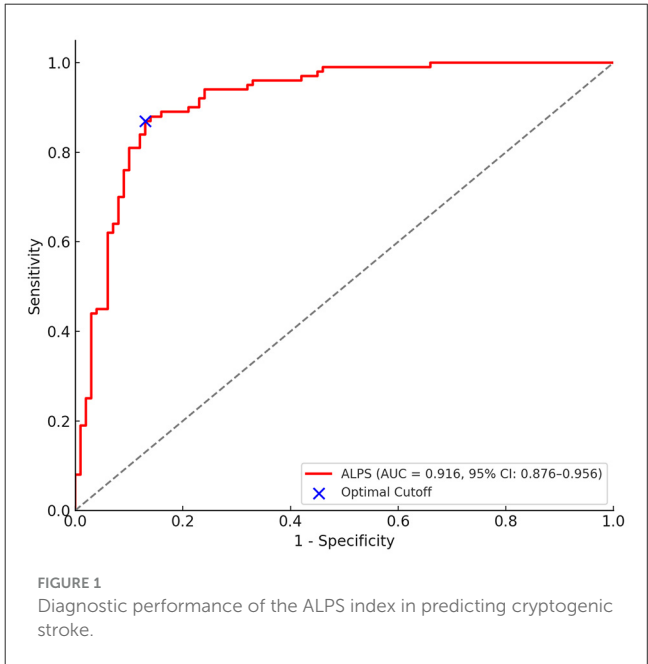
evidence of effect modification. Full estimates are provided in Supplementary Tables S1,S2.

Discussion

In this study, we found that a lower ALPS index, reflecting impaired glymphatic system function, was significantly associated with an increased risk of cryptogenic stroke among PFO patients. The ALPS index demonstrated strong diagnostic performance, with an AUC of 0.916, and remained an independent predictor of cryptogenic stroke after adjustment for clinical confounders. Additionally, longer PFO tunnel length was independently correlated with lower ALPS index values, suggesting a potential link between structural cardiac anomalies and glymphatic dysfunction.

Interestingly, LV EF showed a statistical association with cryptogenic stroke in our model. However, this finding is counterintuitive from a biological standpoint, as higher ejection fraction is generally protective. We consider this association to be spurious, likely reflecting residual confounding or collinearity with other clinical variables, rather than a true causal effect. Thus, it should be interpreted with caution and requires validation in larger, independent cohorts.
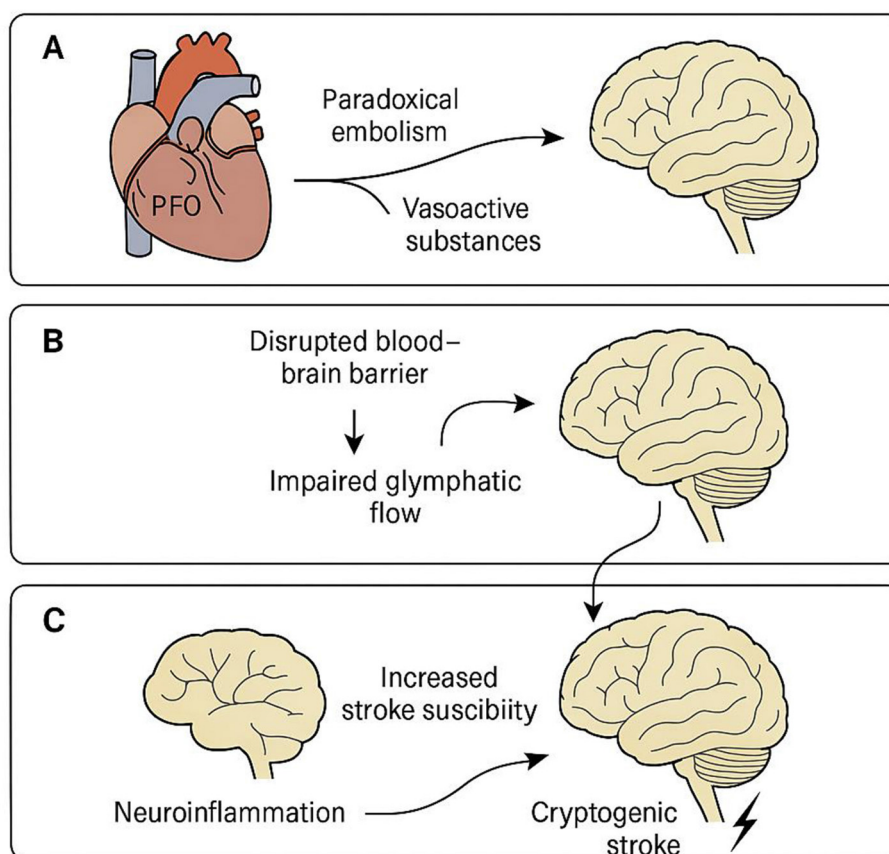
FIGURE 2
Proposed mechanisms linking patent foramen ovale to cryptogenic stroke via glymphatic dysfunction. Schematic representation of the hypothesized pathophysiological pathways by which a patent foramen ovale (PFO) may contribute to cryptogenic stroke through glymphatic system dysfunction. **(A)** Paradoxical embolism and vasoactive substances (e.g., serotonin, CGRP) bypass pulmonary filtration via PFO and enter cerebral circulation. **(B)** These circulating factors disrupt the blood–brain barrier and impair perivascular cerebrospinal fluid (CSF) flow, leading to reduced glymphatic clearance. **(C)** Glymphatic dysfunction promotes neuroinflammation and the accumulation of neurotoxic metabolites, ultimately increasing susceptibility to ischemic injury and stroke. This central illustration highlights the interaction between embolic and clearance-based mechanisms in the pathogenesis of PFO-related cryptogenic stroke.

Epidemiological studies have shown that the prevalence of PFO is ∼61% among patients with cryptogenic stroke, compared to 19% in patients with ischemic stroke of determined etiology (42). Consistently, in the present study, we found that the prevalence of cryptogenic stroke among PFO patients was 25% (52 out of 208 cases), further supporting the strong association between PFO and cryptogenic stroke. Several mechanisms have been extensively studied in the pathogenesis of PFO-related stroke, including paradoxical embolism, *in situ* thrombus formation, atrial structural and hemodynamic abnormalities, and the presence of interatrial septal aneurysm (43, 44). Furthermore, in patients with a history of cryptogenic vascular events, randomized trials have demonstrated that percutaneous PFO closure significantly reduces the risk of recurrent stroke and transient ischemic attack compared to medical therapy alone (45). Percutaneous closure has been shown to be superior to medical therapy in preventing stroke recurrence (46, 47).

Fluid-attenuated inversion recovery sequences were used to identify stroke lesions and other brain abnormalities (30, 48). DTI-ALPS a technique based on DTI, was employed as a non-invasive method to evaluate glymphatic system activity, which

had been demonstrated good stability and excellent interobserver reliability (49–51). Previous studies have demonstrated that PFO is associated with an increased burden of EPVS, reflecting potential glymphatic dysfunction (32). Moreover, structural and hemodynamic abnormalities related to PFO have been implicated in cerebral ischemia and impaired waste clearance (32, 33). Similarly, in our study, we found that patients with PFO had significantly lower ALPS index values compared to controls, indicating impaired glymphatic system function. Furthermore, the lower ALPS index was independently associated with an increased risk of cryptogenic stroke. On the other hand, glymphatic impairment has been increasingly implicated in the pathophysiology of stroke (52, 53). In subarachnoid hemorrhage models, fibrinogen and other blood components have been observed accumulating in enlarged perivascular spaces, accompanied by reduced perivascular AQP4 expression and marked neuroinflammatory responses (54–56). Research further revealed impaired glymphatic inflow and delayed contrast clearance compared to controls (57), along with increased total and phosphorylated tau levels, suggesting compromised waste clearance (58). Restoration of perivascular flow with

tissue-type plasminogen activator partially improved glymphatic function (59). Similarly, ischemic stroke models show perivascular space dilation, loss of AQP4 polarity, and astrocyte activation around infarcts (60). These findings collectively suggest that glymphatic dysfunction may play a critical role in mediating brain injury and impaired recovery following both hemorrhagic and ischemic stroke.

We found that impaired glymphatic function, as indicated by a reduced ALPS index, was identified as an independent risk factor for cryptogenic stroke in patients with PFO. Multiple mechanisms may underlie the increased stroke risk in PFO patients. The paradoxical embolism hypothesis proposes that venous thrombi bypass pulmonary filtration and enter cerebral circulation via the PFO, leading to focal ischemia and blood–brain barrier disruption. This process can independently initiate or aggravate glymphatic dysfunction (61–64). In contrast, a neuroinflammatory and clearance dysfunction model posits that hemodynamic disturbances, hypoxia, and unfiltered vasoactive substances (e.g., serotonin, CGRP) may disrupt CSF–interstitial fluid exchange, compromise glymphatic flow, and promote accumulation of neurotoxic metabolites (65–67). Third, vasoactive and inflammatory substances, such as serotonin (5-HT) and calcitonin gene-related peptide (CGRP), which would normally be filtered by the pulmonary circulation, may directly access the cerebral vasculature, promoting neuroinflammation and vascular injury (68–70). Fourth, hemodynamic alterations associated with PFO may increase circulatory resistance, facilitate microthrombus formation, and aggravate BBB damage (71). These pathways may be synergistic, with PDE triggering ischemia while glymphatic failure impairs post-injury clearance, ultimately amplifying stroke risk (72–74). Although the ALPS index demonstrated strong discriminative performance in our cohort, this finding may partly reflect overfitting. External validation in larger, independent, multicenter datasets is required to confirm its robustness and generalizability.

In our cohort, ISA was significantly more common in patients with cryptogenic stroke compared to controls (55.7% vs. 30.1%), consistent with its established role as a marker of high-risk PFO. However, ISA did not retain statistical significance in the multivariate regression analysis. This discrepancy may reflect model instability given the modest sample size, and possible collinearity between ISA, PFO structural parameters, and the ALPS index. It is plausible that ISA contributes to stroke risk primarily through embolic pathways, whereas ALPS index captures the clearance-related dimension, leading to partial overlap in explanatory power. Thus, ISA should still be considered a clinically important risk factor, even though it did not emerge as an independent predictor in our adjusted model.

Beyond mechanistic insights, the clinical application of the ALPS index may offer valuable utility in risk stratification. As a non-invasive biomarker of glymphatic dysfunction, the ALPS index could help identify PFO patients at elevated risk of stroke who might benefit from more aggressive management, including early consideration of percutaneous closure. Conversely, patients with preserved glymphatic function might be suitable for conservative monitoring. Integrating ALPS index measurements into clinical workflows could thus complement traditional assessments (e.g.,

ROPE score, shunt grade) to refine individualized decision-making for stroke prevention.

Our findings support an association between impaired glymphatic function, as reflected by a lower ALPS index, and stroke occurrence. However, given the cross-sectional design, causality cannot be inferred. It remains unclear whether glymphatic dysfunction predisposes to stroke, or instead represents a consequence of ischemic injury (e.g., AQP4 polarity loss, EPVS dilation). Therefore, longitudinal studies with repeated neuroimaging assessments are essential to clarify temporal directionality. Moreover, prospective validation in larger and more diverse populations is required to determine whether ALPS index can serve as a reliable biomarker for stroke risk stratification.

Study limitations and future direction

Several limitations of this study should be acknowledged. First, the cross-sectional design restricts causal inference. Although a significant association between lower ALPS index and cryptogenic stroke was observed, it remains unclear whether glymphatic dysfunction is a cause or consequence of stroke. Prospective cohort studies or interventional investigations, such as evaluating ALPS index changes after PFO closure, are needed to clarify this relationship. Second, potential selection bias may exist. This was a single-center study, which may limit the generalizability of the findings to broader PFO populations across different regions and ethnicities. In addition, the control group consisted of PFO patients without a history of stroke rather than healthy individuals, which may have led to an underestimation of effect sizes and a shift in baseline ALPS index values. Future studies including healthy controls are warranted to validate and extend our findings. Additionally, the control group consisted of PFO patients without a history of stroke rather than healthy individuals, which may have led to an underestimation of the degree of ALPS index abnormalities. Third, there were methodological limitations related to imaging. While DTI-ALPS is a useful indirect marker of glymphatic function, it does not directly quantify CSF–interstitial fluid exchange rates. Future studies combining DTI-ALPS with advanced imaging modalities, such as dynamic contrast-enhanced MRI or molecular PET imaging, could provide more direct assessments. Fourth, unmeasured confounders may have influenced the results. For example, sleep quality and obstructive sleep apnea (OSA)—both major modulators of glymphatic flow—were not assessed in this study. Furthermore, the use of medications such as statins and antihypertensives, which could influence lipid metabolism, vascular function, and possibly ALPS index values, was not systematically recorded. Finally, microembolic signals (MES) on transcranial Doppler were not measured, which could have provided valuable mechanistic information to help disentangle embolic from clearance-related pathways. Future studies should incorporate these parameters to enhance the mechanistic and clinical interpretability of ALPS index findings in PFO-related cryptogenic stroke. Additionally, the unexpected positive association between LV EF and cryptogenic stroke may reflect collinearity or residual confounding, and should not be

considered as evidence of a causal relationship. Finally, challenges remain regarding clinical translation. The optimal cut-off value for the ALPS index requires validation in larger, multicenter cohorts, and its relationship with stroke recurrence and long-term outcomes was not assessed in this study. Future directions include developing AI-assisted fully automated ALPS index analysis pipelines to enhance reproducibility and integrating 7T MRI and Q-space imaging techniques to achieve submillimeter visualization of glymphatic pathways. Clinical applications may also explore ALPS index-guided PFO management strategies, with more aggressive interventions in patients with impaired glymphatic function.

Conclusions

In summary, among PFO patients, impaired glymphatic function, as indicated by a lower ALPS index, was independently associated with an increased risk of cryptogenic stroke. The ALPS index demonstrated strong discriminative performance in this cohort and may represent a potential imaging biomarker for stroke risk stratification. However, these findings are preliminary and require validation in larger, independent cohorts before translation into clinical practice. These findings highlight the interplay between structural cardiac anomalies and central nervous system clearance dysfunction, offering new insights into the pathophysiology of cryptogenic stroke and potential targets for early risk assessment and intervention.

Data availability statement

The raw data supporting the conclusions of this article will be made available by the authors, without undue reservation.

Ethics statement

The studies involving humans were approved by Fuwai Hospital, Zhengzhou University. The studies were conducted in accordance with the local legislation and institutional requirements. The participants provided their written informed consent to participate in this study. Written informed consent was obtained from the individual(s) for the publication of any potentially identifiable images or data included in this article.

Author contributions

WZ: Data curation, Methodology, Supervision, Conceptualization, Project administration, Investigation, Resources, Visualization, Software, Writing – original draft,

Writing – review & editing. FW: Conceptualization, Formal analysis, Funding acquisition, Investigation, Methodology, Project administration, Resources, Software, Supervision, Validation, Visualization, Writing – original draft, Writing – review & editing. QL: Conceptualization, Writing – original draft.

Conflict of interest

The authors declare that the research was conducted in the absence of any commercial or financial relationships that could be construed as a potential conflict of interest.

Generative AI statement

The author(s) declare that no Gen AI was used in the creation of this manuscript.

Any alternative text (alt text) provided alongside figures in this article has been generated by Frontiers with the support of artificial intelligence and reasonable efforts have been made to ensure accuracy, including review by the authors wherever possible. If you identify any issues, please contact us.

Publisher's note

All claims expressed in this article are solely those of the authors and do not necessarily represent those of their affiliated organizations, or those of the publisher, the editors and the reviewers. Any product that may be evaluated in this article, or claim that may be made by its manufacturer, is not guaranteed or endorsed by the publisher.

Supplementary material

The Supplementary Material for this article can be found online at: https://www.frontiersin.org/articles/10.3389/fneur.2025.1620772/full#supplementary-material

References

1. Chiumente M, Gianino MM, Minniti D, Mattei TJ, Spass B, Kamal KM, et al. Burden of stroke in Italy: an economic model highlights savings arising from reduced disability following thrombolysis. *Int J Stroke.* (2015) 10:849–55. doi: 10.1111/ijs. 12481

2. Kang HY, Lim SJ, Suh HS, Liew D. Estimating the lifetime economic burden of stroke according to the age of onset in South Korea: a cost of illness study. *BMC Public Health.* (2011) 11:646. doi: 10.1186/1471-2458-11-646

3. Gerzeli S, Tarricone R, Zolo P, Colangelo I, Busca MR, Gandolfo C. The economic burden of stroke in Italy. The EcLIPSE study: economic longitudinal incidence-based project for stroke evaluation. *Neurol Sci.* (2005) 26:72–80. doi: 10.1007/s10072-005-0439-0

4. Hamodat O, Almuzainy S, Yahya R, Koniali S. Comparison of patent foramen ovale closure vs medical therapy for the prevention of recurrent cryptogenic stroke: a systematic review. *J Saudi Heart Assoc.* (2025) 37:5. doi: 10.37616/2212-5043.1427

5. Yirmibes EOB, Sengeze N, Gurel B. The frequency of carotid web in cryptogenic stroke and its association with stroke risk factors. *J Stroke Cerebrovasc Dis.* (2025) 34:108295. doi: 10.1016/j.jstrokecerebrovasdis.2025.108295

6. Wadhwa A, Singh RJ, Almekhlafi M, Menon BK, Nambiar PN, Kathuveetil A, et al. Derivation of a CT angiography-based arch atherosclerosis grading in cryptogenic ischemic stroke. *Ann Indian Acad Neurol.* (2025) 28:43–8. doi: 10.4103/aian.aian_996_24

7. Knupp AJ, Smith DA. Increased risk of cryptogenic stroke associated with patent foramen ovale in young adults. *Cureus.* (2024) 16:e53502. doi: 10.7759/cureus.53502

8. Lheritier G, Legras A, Caille A, Lherm T, Mathonnet A, Frat JP, et al. Prevalence and prognostic value of acute cor pulmonale and patent foramen ovale in ventilated patients with early acute respiratory distress syndrome: a multicenter study. *Intensive Care Med.* (2013) 39:1734–42. doi: 10.1007/s00134-013-3017-6

9. Khurana D, Petluri G, Kumar M, Bahl A, Kumar A, Gairolla J, et al. Prevalence of Patent foramen ovale in north indian cryptogenic young strokes. *Neurol India.* (2022) 70:1077–82. doi: 10.4103/0028-3886.349647

10. Randour G, Brassart N, Dagonnier M, Bollens B. Managing anticoagulation and thromboembolic risk in cryptogenic stroke associated with patent foramen ovale. *BMJ Case Rep.* (2025) 18:e264776. doi: 10.1136/bcr-2024-264776

11. Manzoor M, Leskela J, Pietiainen M, Martinez-Majander N, Könönen E, Sinisalo J, et al. Oral microbiome dysbiosis in cryptogenic ischemic stroke patients with high-risk patent foramen ovale. *Sci Rep.* (2025) 15:11535. doi: 10.1038/s41598-025-95728-x

12. Putaala J, Martinez-Majander N, Leppert M, Tulkki L, Pirinen J, Tolppanen H, et al. Burden of modifiable risk factors in young-onset cryptogenic ischemic stroke by high-risk patent foramen ovale. *Stroke.* (2025) 56:1428–40. doi: 10.1161/STROKEAHA.124.049855

13. Bailey CE, Allaqaband S, Bajwa TK. Current management of patients with patent foramen ovale and cryptogenic stroke: our experience and review of the literature. *WMJ.* (2004) 103:32–6.

14. Chessa M, Drago M, Krantunkov P, Bini MR, Butera G, De Rosa G, et al. Differential diagnosis between patent foramen ovale and pulmonary arteriovenous fistula in two patients with previous cryptogenic stroke caused by presumed paradoxical embolism. *J Am Soc Echocardiogr.* (2002) 15:845–6. doi: 10.1067/mje.2002.120289

15. Homma S, Sacco RL, Di Tullio MR, Sciacca RR, Mohr JP, Investigators PFOiCSS. Effect of medical treatment in stroke patients with patent foramen ovale: patent foramen ovale in cryptogenic stroke study. *Circulation.* (2002) 105:2625–31. doi: 10.1161/01.CIR.0000017498.88393.44

16. Martinez-Majander N, Kutal S, Ylikotila P, Yesilot P, Tulkki L, Zedde M, et al. Association between heavy alcohol consumption and cryptogenic ischaemic stroke in young adults: a case-control study. *J Neurol Neurosurg Psychiatry.* (2025) 96:114–21. doi: 10.1136/jnnp-2024-333759

17. Amini T. Cryptogenic stroke and patent foramen ovale: endeavoring for clarity. *Front Neurol.* (2024) 15:1533232. doi: 10.3389/fneur.2024.1533232

18. Shen H, Zhu B, Qian Y, Jin J, Zhou J, Peng G, et al. Advances in research on meningeal lymphatic vessels in central nervous system diseases. *J Craniofac Surg.* (2024). doi: 10.1097/SCS.0000000000010872

19. Gao M, Wang X, Su S, Feng W, Lai Y, Huang K, et al. Meningeal lymphatic vessel crosstalk with central nervous system immune cells in aging and neurodegenerative diseases. *Neural Regen Res.* (2025) 20:763–78. doi: 10.4103/NRR.NRR-D-23-01595

20. Gonuguntla S, Herz J. Unraveling the lymphatic system in the spinal cord meninges: a critical element in protecting the central nervous system. *Cell Mol Life Sci.* (2023) 80:366. doi: 10.1007/s00018-023-05013-1

21. Licastro E, Pignataro G, Iliff JJ, Xiang Y, Lo EH, Hayakawa K, et al. Glymphatic and lymphatic communication with systemic responses during physiological and pathological conditions in the central nervous system. *Commun Biol.* (2024) 7:229. doi: 10.1038/s42003-024-05911-5

22. Li X, Qi L, Yang D, Hao S, Zhang F, Zhu X, et al. Meningeal lymphatic vessels mediate neurotropic viral drainage from the central nervous system. *Nat Neurosci.* (2022) 25:577–87. doi: 10.1038/s41593-022-01063-z

23. Xu JQ, Liu QQ, Huang SY, Duan C-Y, Lu H-B, Cao Y, et al. The lymphatic system: a therapeutic target for central nervous system disorders. *Neural Regen Res.* (2023) 18:1249–56. doi: 10.4103/1673-5374.355741

24. Caballero CA, Cebrian FY, Parra Salinas IM. Infiltration of the central nervous system in patients with chronic lymphatic leukemia. *Med Clin (Barc).* (2023) 161:361–2. doi: 10.1016/j.medcle.2023.09.007

25. Noe FM, Marchi N. Central nervous system lymphatic unit, immunity, and epilepsy: is there a link? *Epilepsia Open.* (2019) 4:30–9. doi: 10.1002/epi4.12302

26. Tamura R, Yoshida K, Toda M. Current understanding of lymphatic vessels in the central nervous system. *Neurosurg Rev.* (2020) 43:1055–64. doi: 10.1007/s10143-019-01133-0

27. Li W, Chen D, Liu N, Luan Y, Zhu S, Wang H. Modulation of lymphatic transport in the central nervous system. *Theranostics.* (2022) 12:1117–31. doi: 10.7150/thno.66026

28. Taoka T. In reply: the improvement technique for reproducibility of diffusion tensor image analysis along the perivascular space (DTI-ALPS) for evaluating interstitial fluid diffusivity and glymphatic function. *Jpn J Radiol.* (2023) 41:1031–2. doi: 10.1007/s11604-023-01431-0

29. Hsiao WC, Chang HI, Hsu SW, et al. Association of cognition and brain reserve in aging and glymphatic function using diffusion tensor image-along the perivascular space (DTI-ALPS). *Neuroscience.* (2023) 524:11–20. doi: 10.1016/j.neuroscience.2023.04.004

30. Gumeler E, Aygun E, Tezer FI, Saritas EU, Oguz KK. Assessment of glymphatic function in narcolepsy using DTI-ALPS index. *Sleep Med.* (2023) 101:522–7. doi: 10.1016/j.sleep.2022.12.002

31. Song H, Ruan Z, Gao L, Lv D, Sun D, Li Z, et al. Structural network efficiency mediates the association between glymphatic function and cognition in mild VCI: a DTI-ALPS study. *Front Aging Neurosci.* (2022) 14:974114. doi: 10.3389/fnagi.2022.974114

32. Liu Y, Li Y, Shang Q, Cao J, Zhao W, Xin J, et al. Increased burden of enlarged perivascular spaces in patients with patent foramen ovale. *Neuroradiology.* (2025) 67:57–64. doi: 10.1007/s00234-024-03532-7

33. Sun L, Cui K, Hu J, Dong L, Liu L, Jia J, et al. Impaired glymphatic system in patent foramen ovale based on diffusion tensor imaging analysis along the perivascular space. *Quant Imaging Med Surg.* (2025) 15:2987–99. doi: 10.21037/qims-24-1963

34. Kolominsky-Rabas PL, Weber M, Gefeller O, Neundoerfer B, Heuschmann PU. Epidemiology of ischemic stroke subtypes according to TOAST criteria: incidence, recurrence, and long-term survival in ischemic stroke subtypes: a population-based study. *Stroke.* (2001) 32:2735–40. doi: 10.1161/hs1201.100209

35. Goldstein LB, Jones MR, Matchar DB, Edwards LJ, Hoff J, Chilukuri V, et al. Improving the reliability of stroke subgroup classification using the Trial of ORG 10172 in Acute Stroke Treatment (TOAST) criteria. *Stroke.* (2001) 32:1091–8. doi: 10.1161/01.STR.32.5.1091

36. Cambise N, Tremamunno S, Marino AG, Lenci L, De Benedetto F, Belmusto A, et al. Transthoracic echocardiography in assessing patients with suspected infective endocarditis (TEASE): an exploratory study. *J Clin Med.* (2025) 14. doi: 10.3390/jcm14072195

37. Rubin MN, Shah R, Devlin T, Youn TS, Waters MF, Volpi JJ, et al. Robot-assisted transcranial doppler versus transthoracic echocardiography for right to left shunt detection. *Stroke.* (2023) 54:2842–50. doi: 10.1161/STROKEAHA.123.043380

38. Zhang H, Huang W, Lan T, Zhang M, Yang J, Zhang H, et al. The value of contrast-enhanced transesophageal echocardiography in the detection of cardiac right-to-left shunt related with cryptogenic stroke and migraine. *Biomed Res Int.* (2020) 2020:8845652. doi: 10.1155/2020/8845652

39. Yue L, Zhai YN, Wei LQ. Which technique is better for detection of right-to-left shunt in patients with patent foramen ovale: comparing contrast transthoracic echocardiography with contrast transesophageal echocardiography. *Echocardiography.* (2014) 31:1050–5. doi: 10.1111/echo.12523

40. Yeh YL, Liu CK, Chang WK, Chan KH Li JY, Tsai SK. Detection of right to left shunt by transesophageal echocardiography in a patient with postoperative hypoxemia. *J Formos Med Assoc.* (2006) 105:418–21. doi: 10.1016/S0929-6646(09)60139-X

41. Hamzehloo A, Mousavi SA. Contrast transcranial Doppler compared to transesophageal echocardiography in detection of right-to-left shunt. *Neurosciences.* (2006) 11:167–70.

42. Cramer SC, Rordorf G, Maki JH, Kramer LA, Grotta JC, Burgin WS, et al. Increased pelvic vein thrombi in cryptogenic stroke: results of the Paradoxical Emboli from Large Veins in Ischemic Stroke (PELVIS) study. *Stroke.* (2004) 35:46–50. doi: 10.1161/01.STR.0000106137.42649.AB

43. Khattab AA, Windecker S, Juni P, Hildick-Smith D, Dudek D, Andersen HR, et al. Randomized clinical trial comparing percutaneous closure of patent foramen ovale (PFO) using the Amplatzer PFO Occluder with medical treatment in patients with cryptogenic embolism (PC-Trial): rationale and design. *Trials.* (2011) 12:56. doi: 10.1186/1745-6215-12-56

44. Kanthan A, Looi KL, Mottram P, Harper R, Bittinger L, Alison JF. Percutaneous left atrial appendage closure using a PFO closure device. *Heart Lung Circ.* (2013) 22:784–5. doi: 10.1016/j.hlc.2013.04.118

45. Kasner SE, Rhodes JF, Andersen G, Iversen HK, Nielsen-Kudsk JE, Settergren M, et al. Five-year outcomes of PFO closure or antiplatelet therapy for cryptogenic stroke. *N Engl J Med.* (2021) 384:970–1. doi: 10.1056/NEJMc2033779

46. Yu J, Liu X, Zhou J, Xue X, Muenzel M, Schulze PC, et al. Long-term safety and efficacy of combined percutaneous LAA and PFO/ASD closure: a single-center experience (LAAC combined PFO/ASD closure). *Expert Rev Med Devices.* (2019) 16:429–35. doi: 10.1080/17434440.2019.1604216

47. von Bardeleben RS, Richter C, Otto J, Himmrich L, Schnabel R, Kampmann C, et al. Long term follow up after percutaneous closure of PFO in 357 patients with paradoxical embolism: difference in occlusion systems and influence of atrial septum aneurysm. *Int J Cardiol.* (2009) 134:33–41. doi: 10.1016/j.ijcard.2008.02.031

48. Liu H, Yang S, He W, Liu X, Sun S, Wang S, et al. Associations among diffusion tensor image along the perivascular space (DTI-ALPS), enlarged perivascular space (ePVS), and cognitive functions in asymptomatic patients with carotid plaque. *Front Neurol.* (2021) 12:789918. doi: 10.3389/fneur.2021.789918

49. Saito Y, Kamagata K, Uchida W, Takabayashi K, Aoki S. Improved reproducibility of diffusion tensor image analysis along the perivascular space (DTI-ALPS) index calculated by manual and automated methods. *Jpn J Radiol.* (2023) 41:1033–4. doi: 10.1007/s11604-023-01429-8

50. Saito Y, Kamagata K, Andica C, Uchida W, Takabayashi K, Yoshida S, et al. Glymphatic system impairment in corticobasal syndrome: diffusion tensor image analysis along the perivascular space (DTI-ALPS). *Jpn J Radiol.* (2023) 41:1226–35. doi: 10.1007/s11604-023-01454-7

51. Yang DX, Sun Z, Yu MM, Zou QQ, Li PY, Zhang JK, et al. Associations of MRI-derived glymphatic system impairment with global white matter damage and cognitive impairment in mild traumatic brain injury: a DTI-ALPS study. *J Magn Reson Imaging.* (2024) 59:639–47. doi: 10.1002/jmri.28797

52. Toh CH, Siow TY. Glymphatic dysfunction in patients with ischemic stroke. *Front Aging Neurosci.* (2021) 13:756249. doi: 10.3389/fnagi.2021.756249

53. Zhou X, Li Y, Lenahan C, Ou Y, Wang M, He Y. Glymphatic system in the central nervous system, a novel therapeutic direction against brain edema after stroke. *Front Aging Neurosci.* (2021) 13:698036. doi: 10.3389/fnagi.2021.698036

54. Lin L, Hao X, Li C, Sun C, Wang X, Yin L, et al. Impaired glymphatic system in secondary degeneration areas after ischemic stroke in rats. *J Stroke Cerebrovasc Dis.* (2020) 29:104828. doi: 10.1016/j.jstrokecerebrovasdis.2020.104828

55. Ji C, Yu X, Xu W, Lenahan C, Tu S, Shao A. The role of glymphatic system in the cerebral edema formation after ischemic stroke. *Exp Neurol.* (2021) 340:113685. doi: 10.1016/j.expneurol.2021.113685

56. Lv T, Zhao B, Hu Q, Zhang X. The glymphatic system: a novel therapeutic target for stroke treatment. *Front Aging Neurosci.* (2021) 13:689098. doi: 10.3389/fnagi.2021.689098

57. Gaberel T, Gakuba C, Goulay R, Martinez De Lizarrondo S, Hanouz JL, Emery E, et al. Impaired glymphatic perfusion after strokes revealed by contrast-enhanced MRI: a new target for fibrinolysis? *Stroke.* (2014) 45:3092–6. doi: 10.1161/STROKEAHA.114.006617

58. Pu T, Zou W, Feng W, Zhang Y, Wang L, Wang H, et al. Persistent malfunction of glymphatic and meningeal lymphatic drainage in a mouse model of subarachnoid hemorrhage. *Exp Neurobiol.* (2019) 28:104–18. doi: 10.5607/en.2019.28.1.104

59. Luo C, Yao X, Li J, He B, Liu Q, Ren H, et al. Paravascular pathways contribute to vasculitis and neuroinflammation after subarachnoid hemorrhage independently of glymphatic control. *Cell Death Dis.* (2016) 7:e2160. doi: 10.1038/cddis.2016.63

60. Wang M, Ding F, Deng S, Guo X, Wang W, Iliff JJ, et al. Focal solute trapping and global glymphatic pathway impairment in a murine model of multiple microinfarcts. *J Neurosci.* (2017) 37:2870–7. doi: 10.1523/JNEUROSCI.2112-16.2017

61. Boberg E, Hedman A, Hollenberg J. Pulmonary embolism with paradoxical embolization to right coronary artery in the presence of a large patent foramen ovale: a case report. *Eur Heart J Case Rep.* (2024) 8:ytae133. doi: 10.1093/ehjcr/ytae133

62. Do AP, Nguyen HM, Thi Thu Nguyen H, Ta CM, Bui STT, Pham HM. Recurrent paradoxical cerebral embolism caused by a thrombus entrapped in a patent foramen ovale: a case report. *Ann Med Surg (Lond).* (2023) 85:5765–9. doi: 10.1097/MS9.0000000000001343

63. Stefan G, Badea AM, Spataru D, Stancu S. Paradoxical renal embolization via patent foramen ovale: a case of complicated pulmonary embolism and renal infarction mitigated by accessory renal arteries (Nephrology images). *J Nephrol.* (2023) 36:2645–7. doi: 10.1007/s40620-023-01722-9

64. Mojaddedi S, Jamil D, Mojadidi MK, Patel NK. Patent foramen Ovale-related paradoxical embolism after noncardiac surgery. *J Cardiol Cases.* (2023) 27:113–5. doi: 10.1016/j.jccase.2022.11.001

65. Donmez-Demir B, Yemisci M, Uruk G, Söylemezoglu F, Bolbos R, Kazmi S, et al. Cortical spreading depolarization-induced constriction of penetrating arteries can cause watershed ischemia: a potential mechanism for white matter lesions. *J Cereb Blood Flow Metab.* (2023) 43:1951–66. doi: 10.1177/0271678X231186959

66. Mehra A, Gomez F, Bischof H, Diedrich D, Laudanski K. Cortical spreading depolarization and delayed cerebral ischemia; rethinking secondary neurological injury in subarachnoid hemorrhage. *Int J Mol Sci.* (2023) 24. doi: 10.3390/ijms24129883

67. Kao YC Li W, Lai HY, Oyarzabal EA, Lin W, Shih YY. Dynamic perfusion and diffusion MRI of cortical spreading depolarization in photothrombotic ischemia. *Neurobiol Dis.* (2014) 71:131–9. doi: 10.1016/j.nbd.2014.07.005

68. Tanaka T, Mori M, Sekino M, Higashijima U, Takaki M, Yamashita Y, et al. Impact of plasma 5-hydroxyindoleacetic acid, a serotonin metabolite, on clinical outcome in septic shock, and its effect on vascular permeability. *Sci Rep.* (2021) 11:14146. doi: 10.1038/s41598-021-93649-z

69. Zullino S, Simoncini T. Impact of selective serotonin reuptake inhibitors (SSRIs) during pregnancy and lactation: a focus on short and long-term vascular effects. *Vascul Pharmacol.* (2018) 108:74–6. doi: 10.1016/j.vph.2018.05.008

70. Snider MA, Harmon DL, Klotz JL. Pharmacologic assessment of bovine ruminal and mesenteric vascular serotonin receptor populations. *J Anim Sci.* (2018) 96:1570–8. doi: 10.1093/jas/sky038

71. Zhu J, Chen A, Zhu L, Li Y, Jiang Z, Ni D, et al. Right atrial septal in situ microthrombus: a potential novel cause of patent foramen ovale-associated stroke. *J Am Heart Assoc.* (2024) 13:e035838. doi: 10.1161/JAHA.124.035838

72. Niiyama S, Ueno Y, Kurita N, Nakajima S, Kijima C, Hira K, et al. White matter lesions as a prognostic marker of recurrence in cryptogenic stroke with high-risk patent foramen ovale. *J Stroke Cerebrovasc Dis.* (2024) 33:108048. doi: 10.1016/j.jstrokecerebrovasdis.2024.108048

73. Putaala J, von Sarnowski B, Schminke U, Busch R, Martinez-Majander N, Ylikotila P, et al. Association of hypertension with early-onset cryptogenic ischemic stroke by the presence of patent foramen ovale: a case-control study. *J Am Heart Assoc.* (2024) 13:e036254. doi: 10.1161/JAHA.124.036254

74. Rengel AC, Gericke C. Embolic ischemic cortical stroke in a young flight instructor with a small patent foramen ovale. *Aerosp Med Hum Perform.* (2024) 95:784–7. doi: 10.3357/AMHP.6483.2024